Heavy-quark thresholds in Higgs-boson physics

Manuel Drees

CERN, CH-1211 Geneva 23, Switzerland

Ken-ichi Hikasa

National Laboratory for High Energy Physics (KEK), Tsukuba-shi, Ibaraki 305, Japan

(Received 30 May 1989)

We perform a comprehensive study of the effects related to a heavy-quark threshold in the production and decay of a scalar or pseudoscalar Higgs particle. We study the QCD corrections to the decay mode into a quark-antiquark pair and also the mixing of a Higgs boson with quarkonium states, both below and above the open-flavor threshold, which can change the properties of the Higgs boson drastically. Numerical results for a Higgs boson of mass around 10 GeV, where the mixing with $b\bar{b}$ states has a great influence on the decay widths and branching ratios, are worked out in detail for the cases of the standard model and minimal supersymmetry. The production cross section of a Higgs particle can also be enhanced by mixing with a quarkonium. A possibility to search for a Higgs boson in the 10-GeV mass range via $\tau^+\tau^-$ decays in fixed-target pp experiments at the Fermilab Tevatron or Serpukhov UNK is suggested, and ways to enhance the signal-to-background ratio are discussed.

I. INTRODUCTION

Perhaps the greatest challenge to contemporary high-energy physics is to find ways to detect the Higgs boson(s) thought to be responsible for the spontaneous breakdown of the $SU(2) \times U(1)_Y$ gauge symmetry of the standard model (SM). To achieve this goal a good understanding of the production and decay properties of Higgs boson(s) is of crucial importance, and much work has been done[1] along these lines.

In general all Higgs bosons couple most strongly to the heaviest particles; they thus tend to decay into the heaviest possible particles. This is even true when the phase space for this decay mode is fairly small. This shows that threshold effects can be very important in Higgs-boson physics. These effects can easily be computed for Higgs-boson decays into heavy leptons or weak gauge bosons; the main effect is the appropriate S- or P-wave phase-space suppression. However, the situation is much more complicated for Higgs-boson decays into a heavy-quark–antiquark pair. In this paper we attempt to give a comprehensive description of effects that occur around such a heavy-quark threshold.

Three distinct effects can be distinguished. First, when approaching the heavy-quark threshold from above, strong radiative corrections[2] to the Higgs boson $\to q\bar{q}$ decay width tend to become very large. In fact, the correction factor has a $1/\beta$ singularity, where β is the velocity of the heavy quark in the Higgs-boson rest frame. Very close to threshold one would clearly have to sum an infinite series of perturbative corrections proportional to $(\alpha_s/\beta)^n$, corresponding to n-gluon exchange between the quark and the antiquark. As shown by Schwinger[3] for the case of QED, this is equivalent to the use of a $1/r$ potential to describe the interactions between the quark and the antiquark. For the case of QCD it is known[4] that the relevant potential is more complicated. In any case, one

finally ends up with a Higgs boson interacting not with a "free" $q\bar{q}$ pair, but with a $q\bar{q}$ bound state. Of course, this interaction can no longer manifest itself in a Higgs boson $\to q\bar{q}$ decay; instead, the Higgs boson *mixes*[5] with $q\bar{q}$ bound states with the appropriate quantum numbers. This is the second effect associated with heavy-quark thresholds. As we will show in Sec. II A it can be important in quite a wide region below the open-flavor threshold.

Both the mixing with bound states below the open flavor threshold and the QCD corrections somewhat above this threshold rest on rather firm theoretical ground. The situation is much less clear just above the threshold, where the hadronization of the heavy quarks is of crucial importance. The hadronization even affects the purely kinematical threshold factor: While a parity-even Higgs boson has to decay into a P-wave $q\bar{q}$ pair, the resulting pseudoscalar mesons carrying q flavor (e.g., B mesons for $q = b$) can be in S wave. Also, the difference between the quark mass, defined as the pole of the "free" quark propagator, and the mass of the lightest q-flavored mesons becomes important. In this paper we propose to describe these effects by assuming that right above the open-flavor threshold, the decay of the Higgs boson into this open flavor is dominated by the mixing of the Higgs boson with $q\bar{q}$ *resonance* states. In Sec. II B we will describe a simplified model for this mixing.

So far we have only discussed the decay of Higgs bosons. In Sec. III we show that the mixing of Higgs bosons with $q\bar{q}$ bound states can greatly increase the Higgs-boson cross section via gluon fusion. Indeed, if a scalar or pseudoscalar Higgs boson has a mass of about 10 GeV, the $pp \to gg \to$ Higgs boson $\to \tau^+\tau^-$ signal might be observable in Fermilab Tevatron and Serpukhov UNK fixed-target experiments.

Although the SM contains only one physical Higgs boson which has scalar couplings to fermions, in almost all

extensions of this minimal structure one finds at least one Higgs boson with pseudoscalar couplings. One notable example is the Higgs sector of minimal supersymmetry,[6] within the framework of which we will work throughout this paper. The reasons for this are the following. First, the Higgs sector of the SM is known to be technically unnatural; this problem can be remedied by the introduction of space-time supersymmetry. Second, and for the purpose of this paper perhaps more importantly, it is a simple Higgs sector which allows us to introduce both scalar and pseudoscalar Higgs boson without a proliferation of parameters. For the convenience of the reader we give a brief description of this model in Appendix A. It should be noted that our results are directly applicable also to the minimal Higgs boson in the SM, and in fact we will show some results for SM couplings.

Finally, whenever we present numerical results we choose $q = b$. Again we have two reasons for this. First, Higgs bosons with masses around 10 GeV will soon be accessible[7] at the CERN e^+e^- collider LEP and the SLAC Linear Collider (SLC), and might even now be accessible at the KEK e^+e^- collider TRISTAN[8] and the Tevatron; our results are thus of immediate relevance. Second, we can use the experimental data on the Υ and χ_b states to sharpen our predictions. In Appendix B we briefly describe how we treated the mixing between the Higgs bosons and the multitude of $b\bar{b}$ bound states and resonances.

II. HIGGS-BOSON DECAYS IN THE THRESHOLD REGION

In this section we discuss heavy-quark threshold effects on the decay of a scalar Higgs boson H and a pseudoscalar Higgs boson P. As mentioned in the Introduction we work in the framework of minimal supersymmetry. Some details of the Higgs sector are reviewed in Appendix A. Note that the entire Higgs sector is fixed by the values of two parameters, which can be chosen to be the mass of the pseudoscalar P, and the ratio $\omega = \bar{v}/v$ of the vacuum expectation values of the two neutral Higgs fields. Up-quark masses are proportional to $\bar{v}$, so that usually $\omega \geq 1$ can be assumed. In our numerical examples we often have $m_P^2 \ll m_Z^2$; in this case the mass of the scalar Higgs boson is approximately given by (see Appendix A)

$$m_H \simeq m_P \left| \frac{\omega^2 - 1}{\omega^2 + 1} \right| ,$$

i.e., $m_H \leq m_P$ always. Note furthermore that in the limit $\omega^2 \gg 1$, the coupling constants of H and P to quarks and leptons become identical. We now turn to a discussion of Higgs-boson decays below (Sec. II A) and above (Sec. II B) the open-flavor threshold.

A. Below the open-flavor threshold

Even though the Higgs boson $\to q\bar{q}$ decay is kinematically forbidden in this region, the presence of the heavy quark q can become relevant through mixing between the

Higgs boson and $q\bar{q}$ bound states with matching quantum numbers; see Fig. 1. The parity-even, scalar Higgs boson H can mix[5] with the $J = 0$ member of the P-wave spin triplet states, usually called χ_0, whereas the parity-odd, pseudoscalar P can mix with S-wave spin-singlet states called η. This mixing can be described by the introduction of off-diagonal elements in the H-χ_0 and P-η mass matrices; following the notation of Ref. 9 we denote these off-diagonal elements by δm_H^2 and δm_P^2, respectively. Within the framework of nonrelativistic potential models, they can readily be computed from the diagram of Fig. 1:

$$\delta m_H^2 = C_{Hq\bar{q}} \left[\frac{27\sqrt{2}}{\pi} G_F m_\chi \right]^{1/2} |R'(0)| , \tag{2.1a}$$

$$\delta m_P^2 = C_{Pq\bar{q}} \left[\frac{3\sqrt{2}}{4\pi} G_F m_\eta^3 \right]^{1/2} |R(0)| . \tag{2.1b}$$

Here, G_F is the Fermi constant, and $C_{Hq\bar{q}}$ and $C_{Pq\bar{q}}$ arise from mixing between the two Higgs doublets of our model, see Eqs. (A4); finally, $R(0)$ and $R'(0)$ are the S-wave and derivative of the P-wave $q\bar{q}$ wave function at the origin, respectively.

In general it is necessary to include the finite decay widths of both the Higgs bosons and the bound states in the mass matrices, making them non-Hermitian. The total widths of H and P before mixing are to a very good approximation given by the sum of the partial widths for the Higgs boson $\to c\bar{c}$, $\tau^+\tau^-$, and gg decay modes:

$$\Gamma(A \to \tau^+\tau^-) = C_{A\tau\bar{\tau}}^2 \frac{G_F m_\tau^2}{4\sqrt{2}\pi} m_A \left[1 - \frac{4m_\tau^2}{m_A^2} \right]^{l_A}$$
$$(A = H, P) , \tag{2.2}$$

where $l_H = \frac{3}{2}$, $l_P = \frac{1}{2}$;

$$\Gamma(A \to c\bar{c}) = C_{Ac\bar{c}}^2 \frac{3G_F m_c^2}{4\sqrt{2}\pi} m_A \left[1 - \frac{4m_c^2}{m_A^2} \right]^{l_A}$$
$$\times \left[1 + \frac{4\alpha_s(m_A^2)}{3\pi} \Delta_A(m_c, m_A) \right] , \tag{2.3}$$

where the functions Δ_A describe the lowest-order QCD corrections:

$$\Delta_H = \frac{1}{\beta} A(\beta) + \frac{1}{16\beta^3}(3 + 34\beta^2 - 13\beta^4)\ln\frac{1+\beta}{1-\beta}$$
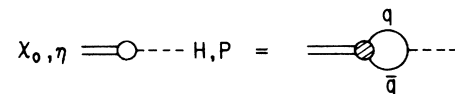$$+ \frac{3}{8\beta^2}(-1 + 7\beta^2) , \tag{2.4a}$$

FIG. 1. Diagrammatical depiction of mixing between a $q\bar{q}$ bound state and an elementary Higgs particle. In the scalar case of H-χ mixing the blob in the Feynman diagram to the right stands for $|R'_\chi(0)|$, and in the pseudoscalar case of P-η mixing for $|R_\eta(0)|$.

$$\Delta_P = \frac{1}{\beta} A(\beta) + \frac{1}{16\beta}(19 + 2\beta^2 + 3\beta^4)\ln\frac{1+\beta}{1-\beta}$$

$$+ \tfrac{3}{8}(7 - \beta^2) \,, \tag{2.4b}$$

where

$$A(\beta) = (1+\beta^2)\left[4\text{Li}_2\left[\frac{1-\beta}{1+\beta}\right] + 2\text{Li}_2\left[-\frac{1-\beta}{1+\beta}\right]\right.$$

$$-3\ln\frac{2}{1+\beta}\ln\frac{1+\beta}{1-\beta}$$

$$\left. -2\ln\beta\ln\frac{1+\beta}{1-\beta}\right]$$

$$-3\beta\ln\frac{4}{1-\beta^2} - 4\beta\ln\beta \,. \tag{2.5}$$

Here $\beta = (1 - 4m_c^2/m_{H,P}^2)^{1/2}$ for Eqs. (2.4a) and (2.4b), respectively, and $\text{Li}_2(x) = -\int_0^x (dt/t)\ln(1-t)$ is the Spence function. Equation (2.4a) has first been derived in Ref. 2; Eq. (2.4b) agrees[10] with Ref. 11. Since we are interested

in the region $m_{H,P} \sim 10$ GeV, the Higgs boson$\rightarrow$ charm decay widths should be adequately described by Eqs. (2.3) and (2.4); for higher Higgs-boson masses it might become necessary to sum[2] the leading-logarithmic corrections, which are identical[12] in Δ_H and Δ_P. Needless to say, the formula (2.3) applies to the decay to any quark pair, $A \rightarrow q\bar{q}$, with the replacement $c \rightarrow q$.

The Higgs boson$\rightarrow gg$ decays can only occur at one loop, but they may nevertheless make important contributions[13] to the total widths. They can be written in the form

$$\Gamma(A \rightarrow gg) = \frac{1}{4\pi m_A}\sum_{\text{pol}}|\mathcal{M}(A \rightarrow gg)|^2 \,, \tag{2.6}$$

where the sum runs[14] over the polarization of the two outgoing gluons, described by the polarization four-vectors ε_1 and ε_2. For the scalar H both quarks and their superpartners contribute; assuming that the left- and right-handed up and down squarks are all degenerate in mass,[15] one finds[13]

$$\mathcal{M}(H \rightarrow gg) = (k_1 \cdot k_2 \varepsilon_1^* \cdot \varepsilon_2^* - k_1 \cdot \varepsilon_2^* k_2 \cdot \varepsilon_1^*)\frac{\alpha_s(m_H^2)}{\pi m_H^2}(\sqrt{2}\, G_F)^{1/2}\sum_{\text{flavors}} m_q^2 C_{Hq\bar{q}}\left\{\left[2 + \left[\frac{4m_q^2}{m_H^2} - 1\right]I\left[\frac{4m_q^2}{m_H^2}\right]\right]\right.$$

$$\left. - \left[2 + \frac{4m_q^2}{m_H^2}I\left[\frac{4m_q^2}{m_H^2}\right]\right]\right\} \,. \tag{2.7a}$$

Here and hereafter the color factor δ_{ab} (a,b being the color indices of the two gluons) is suppressed. For $m_H \sim 10$ GeV, $m_q \gtrsim 70$ GeV (see Ref. 16), one finds that the squark contribution, given by the second square brackets in Eq. (2.7a), is always very small. We used $m_q = 100$ GeV in our numerical calculations. For the pseudoscalar P only quarks can contribute in the loop when $\tilde{q}_L - \tilde{q}_R$ mixing is neglected; one finds[13]

$$\mathcal{M}(P \rightarrow gg) = \varepsilon_{\mu\nu\rho\sigma}k_1^\mu k_2^\nu \varepsilon_1^{*\rho}\varepsilon_2^{*\sigma}\frac{\alpha_s(m_P^2)}{\pi m_P^2}(\sqrt{2}\, G_F)^{1/2}\sum_{\text{flavors}} m_q^2 C_{Pq\bar{q}}I\left[\frac{4m_q^2}{m_P^2}\right] \,, \tag{2.7b}$$

where k_i is the momentum vector of the ith gluon. Finally, the function $I(x)$ appearing in Eqs. (2.7) is given by[17]

$$I(x) = \begin{cases} -2\left[\arctan\dfrac{1}{\sqrt{x-1}}\right]^2, & x \geq 1 \,, \\[2mm] \dfrac{1}{2}\left[\ln\dfrac{x_+}{x_-} - i\pi\right]^2, & 0 < x < 1 \end{cases} \tag{2.8}$$

with $x_\pm = 1 \pm \sqrt{1-x}$. Note that we have been careful to keep the phases of the decay amplitudes (2.7) since they will be crucial to get the correct interference pattern.

For the η and χ_0 bound states we assume that their total decay width is equal to the partial width into two gluons. This is a good approximation for $b\bar{b}$ bound states, but in case of χ_0 may underestimate the width of $t\bar{t}$ bound states[18] or bound states of even heavier fourth-generation quarks[19] by several orders of magnitude. The partial widths for the decays of η and χ_0 into two gluons can again be written in the form of Eq. (2.6) where one now has[20]

$$\mathcal{M}(\chi_0 \rightarrow gg)$$

$$= (k_1 \cdot k_2 \varepsilon_1^* \cdot \varepsilon_2^* - k_1 \cdot \varepsilon_2^* k_2 \cdot \varepsilon_1^*)\frac{16\alpha_s}{m_\chi}\left[\frac{3\pi}{m_\chi^5}\right]^{1/2}|R'(0)| \,, \tag{2.9a}$$

$$\mathcal{M}(\eta \rightarrow gg) = \varepsilon_{\mu\nu\rho\sigma}k_1^\mu k_2^\nu \varepsilon_1^{*\rho}\varepsilon_2^{*\sigma}\frac{8\alpha_s}{m_\eta}\left[\frac{\pi}{3m_\eta^3}\right]^{1/2}|R(0)| \,. \tag{2.9b}$$

Since the relevant bound states dominantly decay into two gluons, it is immediately clear that the largest mixing effects will be seen in the Higgs boson$\rightarrow gg$ decay mode. Consider the simplified case where there is only one η state and one χ_0 state; the physical, mass eigenstates, denoted by the subscript M, are then mixtures of H and χ_0, or P and η:

$$H_M = \frac{1}{N}(H\cos\theta_H + \chi_0\sin\theta_H) \, ,$$

$$\chi_{0M} = \frac{1}{N}(\chi_0\cos\theta_H - H\sin\theta_H) \, ,$$

(2.10)

where $N \equiv (|\cos\theta_H|^2 + |\sin\theta_H|^2)^{1/2} \neq 1$ in general, since θ_H is complex (see Appendix B). The Higgs-boson-like state H_M is defined here as the state with larger Higgs-boson component. The physical states P_M and η_M can be defined analogously. The two-gluon decay amplitudes of the physical states are then given by

$$\mathcal{M}(H_M \to gg) = \frac{1}{N}[\cos\theta_H \mathcal{M}(H \to gg)$$

$$+ \sin\theta_H \mathcal{M}(\chi_0 \to gg)] \, ,$$

(2.11a)

$$\mathcal{M}(\chi_{0M} \to gg) = \frac{1}{N}[\cos\theta_H \mathcal{M}(\chi_0 \to gg)$$

$$- \sin\theta_H \mathcal{M}(H \to gg)] \, ,$$

(2.11b)

and similarly for the P_M, η_M states.

Note that for the $b\bar{b}$ system the gg decay widths of χ and η states are of the order of 1 MeV and a few MeV, respectively, whereas the gg widths of unmixed scalar or pseudoscalar Higgs bosons with a mass around 10 GeV are only a few hundred eV. The second term in Eq. (2.11b) is therefore always negligible; the gg widths of the bound state can thus at most be altered by a factor of 2, and for small mixing the effect is quadratic in θ and thus negligible. In contrast, the $H_M, P_M \to gg$ decay widths can be a thousand times bigger than those of the unmixed states, if the mixing is large.

Before we can present numerical results for the $b\bar{b}$ system we have to fix the masses and wave functions at the origin of the various $b\bar{b}$ bound states. Our choice of parameters is summarized in Tables I(a) and I(b) for the χ_0 and η states, respectively. The masses of the two χ_0 states below the open-bottom threshold[21] are taken directly from experiment.[22] Unfortunately no quantity proportional to $|R'(0)|^2$ has yet been measured; we therefore used the model calculations of Ref. 23, which reproduce other measured parameters of $b\bar{b}$ bound states quite

accurately. None of the six η states has yet been found experimentally. We took the values for the masses of the first three states from the recent calculation of Ref. 24. The wave functions at the origin of the η states are (up to small spin effects) identical to those of the corresponding Υ states, and can therefore be determined from the measured $\Upsilon \to e^+e^-$ decay widths:

$$|R_n(0)|^2 = \Gamma(\Upsilon(n) \to e^+e^-)\frac{9m_{\Upsilon(n)}^2}{4\alpha^2}\left[1 - \frac{16\alpha_s(m_\Upsilon^2)}{3\pi}\right]^{-1} \, ,$$

(2.12)

where we have included first-order QCD corrections[25,26] with[27] $\Lambda = 0.2$ GeV, and the values of the decay widths were taken from the Particle Data Group.[22] Finally, the masses of the last three η states were obtained using the prediction[25,28] of nonrelativistic potential models

$$m_{\Upsilon(n)} - m_{\eta(n)} = K|R_n(0)|^2 \, ,$$

(2.13)

where we have used $K = 6 \times 10^{-3}$ GeV^{-2} to reproduce the masses of the first three η states predicted in Ref. 24. It should be noted that four η states are expected to be below the open-flavor threshold, whereas only three Υ states are below the $B\bar{B}$ threshold. This is because parity (or CP) conservation forbids the decay $\eta \to B\bar{B}$, so that the lowest available open-flavor state for η decay is $B^*\bar{B}$, which lies about 50 MeV higher.

We are now in a position to discuss the mixing of Higgs bosons with $b\bar{b}$ bound states quantitatively. In order to get some feeling for the magnitude of the expected effects we first discuss the simplified case where the Higgs boson mixes with only one bound state. In Fig. 2 we show $\sin2\theta = 2\sin\theta\cos\theta$ for $P - \eta(1)$ and $H - \chi_0(1)$ mixing as a function of the mass difference of the unmixed states, where we have assumed SM coupling strengths for
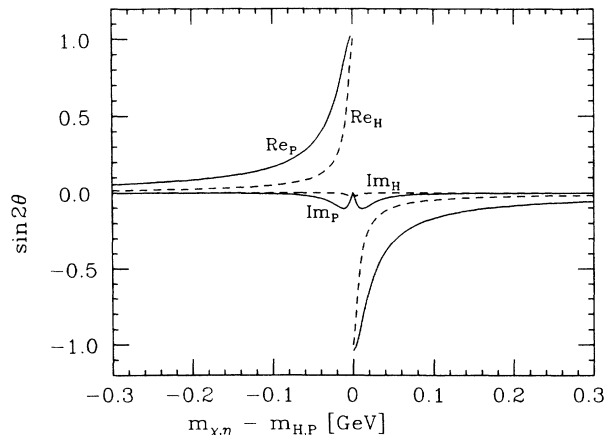
TABLE I. The parameters of spin-0 $b\bar{b}$ bound states.

n	(a) χ_0 states $m_{\chi(n)}$ (GeV)	$\|R_n'(0)\|^2$ (GeV^5)
1	9.860	1.7
2	10.235	2.0

n	(b) η states $m_{\eta(n)}$ (GeV)	$\|R_n(0)\|^2$ (GeV^3)
1	9.412	8.0
2	9.992	3.8
3	10.340	3.0
4	10.570	1.7
5	10.846	2.3
6	11.014	1.0

FIG. 2. The mixing parameter $\sin2\theta = 2\sin\theta\cos\theta$ is plotted as a function of the mass difference between the lowest relevant $b\bar{b}$ bound state and elementary scalars for the case of standard-model coupling strengths of the Higgs bosons (i.e., $\omega = 1$ for the pseudoscalar, $m_P \to \infty$ for the scalar). Real and imaginary parts are shown separately. Note that θ is defined as the complex angle between the physical Higgs-boson-like state and the unmixed Higgs boson.

the Higgs bosons (i.e., $m_P \to \infty$ for the case $m_H \simeq m_{\chi_0(1)}$); we see from Eqs. (2.11) that this quantity determines the magnitude and phase of the interference term in the Higgs boson$\to gg$ decay width. This quantity is given by[9] (see Appendix B for more details)

$$\sin^2 2\theta_H = \frac{(\delta m_H^2)^2}{\frac{1}{4}(m_H^2 - i\Gamma_H m_H - m_{\chi_0}^2 + i\Gamma_{\chi_0} m_{\chi_0})^2 + (\delta m_H^2)^2},$$
(2.14)

where δm_H^2 is given by Eq. (2.1a), and correspondingly for the pseudoscalar mixing angle θ_P. Note the following general features of Fig. 2.

(i) The imaginary part of $\sin 2\theta$ is always much smaller than the real part, although it can reach 0.1 in the pseudoscalar case and is thus not totally negligible. The reason is that both the Higgs bosons and the bound states are quite narrow ($\Gamma < 10$ MeV); this is, however, no longer true for the $b\bar{b}$ resonance states, where the imaginary part does indeed become important.

(ii) At $m_H^2 = m_{\chi_0}^2$, the imaginary part vanishes exactly, as long as $(\Gamma_H m_H - \Gamma_{\chi_0} m_{\chi_0})^2 < (\delta m_H^2)^2$. However, the absolute value of the real part is bigger than one, which shows that θ itself is still complex. Note also that the real part changes sign[29] at $m_H = m_{\chi_0}$. From Eqs. (2.7)–(2.9) one can then derive that the interference in the physical Higgs boson$\to gg$ decay width will be constructive for $m_{H,P} < m_{\chi_0, \eta}$, and destructive otherwise. In the case of a very broad resonance state $(m_\chi \Gamma_\chi > \delta m^2)$ the behavior of real and imaginary parts is interchanged.

(iii) Mixing effects are important over a much larger region of mass splittings in the pseudoscalar case. The reason is simply that the corresponding δm_P^2 is larger than δm_H^2, just like η decay widths into a given final state are bigger than χ decay widths. Even for the pseudoscalar case, however, mixing effects which depend on the deviation of $|\cos\theta|$ from one will be important only if the mass splitting is not more than 50 MeV, at least for the given case $\omega = 1$. On the other hand, the interference term in Eq. (2.11a) (for the pseudoscalar case) will be important for mass differences as large as 300 MeV, since $|\mathcal{M}(\eta \to gg)| \gtrsim 30 |\mathcal{M}(P \to gg)|$. This region can be substantially larger if ω is larger than one, since then the couplings of H and P to $b\bar{b}$ increase in magnitude.

The mixing also induces a small mass shift, which tends to increase the difference between the masses of the physical states. For the below-threshold states the minimal mass difference between "Higgs-boson-like" and "bound-state-like" states is approximately equal to $\delta m_A^2 / m_A$ ($A = H, P$), or (for SM coupling strengths) about 5 MeV for the scalar states, and between 8 and 16 MeV for the pseudoscalar states. These shifts are probably too small to be significant (as deviation from quark-model calculations) in the scalar case; they might be significant for the η states, but these are unfortunately notoriously hard to produce experimentally. Furthermore the mass shift will only be sizable if the masses of the unmixed states are very close. Nevertheless these mass splittings are large enough to guarantee that even if

$m_H = m_\chi$ before mixing, two well-separated γ lines should be visible when the χ state is produced by the radiative decay of higher Υ states. Some small region of $m_H - m_\chi$ may therefore be excluded from existing experiments.

From these considerations it is clear that the most dramatic mixing effects will manifest themselves in the $H, P \to gg$ decay widths, Eqs. (2.9)–(2.11). In Figs. 3(a) and 3(b) we show the predictions for $\Gamma(H \to gg)$ and $\Gamma(P \to gg)$, respectively, with (solid curve) and without (dotted curves) mixing effects, for $\omega = 2$. Obviously all $b\bar{b}$ bound states below the open-flavor threshold can lead to large enhancements of the gluonic width of Higgs bosons, whereas only the pseudoscalar resonances are sufficiently
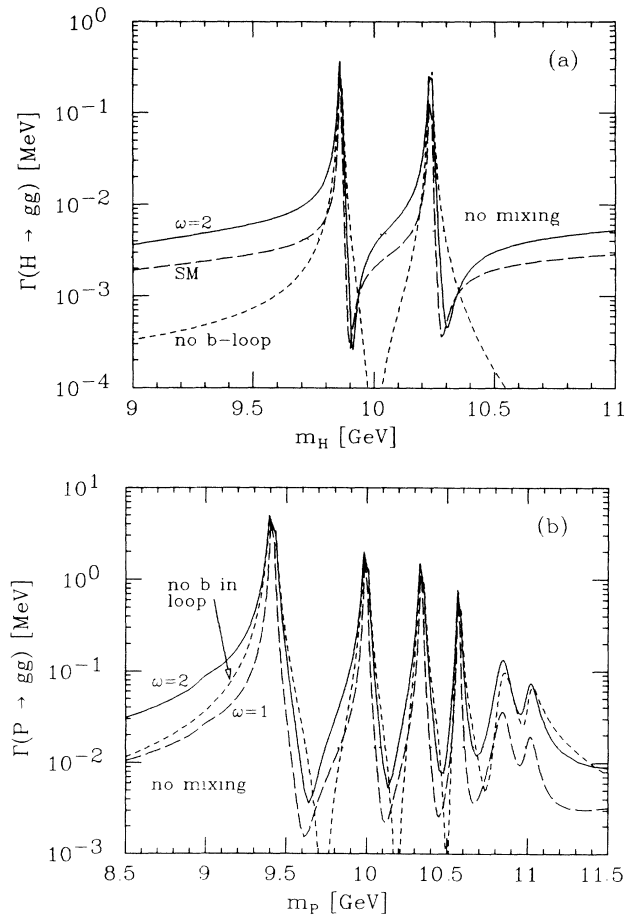
FIG. 3. The gluonic decay width of the scalar (a) and pseudoscalar (b) Higgs bosons close to the $b\bar{b}$ threshold. The dotted curves show the prediction when all mixing effects are neglected, in which case the decay proceeds via quark and (in the scalar case) squark loops, where we have used $m_c = 1.37$ GeV, $m_b = 4.5$ GeV, and $m_{\tilde{q}} = 100$ GeV. The solid and long-dashed curves include mixing effects as well as b-quark contributions to the loop, while the latter have been omitted for the short-dashed curve, which also holds for $\omega = 2$. Note that unlike in the pseudoscalar case, the dotted curve in (a) does not show a kink (which is an artifact of the one-loop approximation) at $m_H = 2m_b = 9$ GeV. The x axis in this figure and in Figs. 4 and 5 is the mass of the physical Higgs-boson-like particle; strictly speaking the curves should therefore have tiny gaps around the positions of the bound states, as discussed in the text.

narrow to produce a peak above the threshold (see following subsection). Just after each maximum one finds a steep drop due to the onset of negative interference between the two terms in Eq. (2.11a), as discussed above. Note that we have used[30] $m_b = 4.5$ GeV in the calculation of the $H, P \rightarrow gg$ loop amplitudes, leading to a substantial imaginary part of the function I [see Eq. (2.8)] and hence a nontrivial phase between the two contributions in Eq. (2.11a); the cancellation is therefore never complete. On the other hand, including both the b-loop contribution and the mixing contribution to the gluonic decay width might be double counting, since the loop integrals are dominated by momenta which allow some quarks in the loop to be nearly on shell, similar to the situation in a bound state. We therefore also show results where we have only allowed c and t quarks (with[30] $m_c = 1.37$ GeV, $m_t = 50$ GeV) in the loop (short-dashed lines, for $\omega = 2$). We see that the effects can be quite dramatic especially for $\omega > 1$, in which case H and P couplings to $c\bar{c}$ and $t\bar{t}$ are suppressed and those to $b\bar{b}$ enhanced, so that the b-quark contribution dominates the $H, P \rightarrow gg$ amplitudes. Since now the loop contributions have only a small imaginary part, the cancellation between the two terms in Eq. (2.11a) can be almost complete; since the loop contributions have been decreased in magnitude, the location of these minima is shifted to the right, toward smaller mixing angles. However, since neglecting the b-quark contribution to the loops is clearly wrong in the limit of small mixing, i.e., large mass differences between Higgs bosons and bound states, whereas for large mixing the physical Higgs boson $\rightarrow gg$ amplitude is in any case dominated by the mixing contribution, we feel that including the b-quark contribution to the loop gives results closer to the correct answer.[31]

For comparison we also show results for SM coupling strengths of the Higgs bosons (long-dashed curves), including b quarks in the $H, P \rightarrow gg$ loops. As anticipated, the regions where mixing is important shrinks, leading to narrower maxima; since the real part of the $P \rightarrow gg$ loop amplitude has been reduced by a factor of 2 compared to the case $\omega = 2$, the minima have also become deeper.

What further measurable effects might be expected from the mixing between Higgs bosons and bound states? Obviously the decay of Higgs bosons into two photons would be affected in a similar fashion as the gluonic decay. However, the branching ratio will always be very small, well below 0.1%, and therefore probably not of interest for Higgs bosons with mass around 10 GeV. The situation might, however, well be different for a heavier Higgs boson mixing with $t\bar{t}$ bound states; if it cannot decay into real W or Z pairs (these decays are always forbidden for pseudoscalars at the lowest order), the $\gamma\gamma$ decay mode might offer the best chance to detect it at hadron supercolliders.[32] Of course, as discussed in Sec. III, the Higgs-boson production cross section from gluon fusion would also be substantially affected by mixing in this case.

All other mixing effects are quadratic in the mixing angle for small mixing, and thus only observable if the mass difference between Higgs boson and bound state is very small; see Fig. 2. The total width of the χ and η states

can be reduced by a factor of 2 in case of maximal mixing. However, since in this case both mixed states would be produced equally, this effect would be very hard to detect, especially since the predictions for gluonic decay widths from leading-order QCD calculations are rather uncertain anyway. An increase in the $\eta, \chi_0 \rightarrow \tau^+ \tau^-$ branching ratio might in principle be easier to measure. For the narrower χ_0 states this branching ratio may be as large as 2% even for $\omega = 1$, if mixing is maximal. However, a sizable $\tau^+ \tau^-$ branching ratio for the χ_0 also implies that a substantial number of Higgs bosons is produced along with the χ_0 from radiative decays of heavier Υ states; since this has not been observed a sizable $\chi_0 \rightarrow \tau^+ \tau^-$ branching ratio is unlikely. We thus conclude that the $H, P \rightarrow gg$ decay width is by far the most promising place to look for mixing effects below the open bottom threshold.

B. Above the open-flavor threshold

Because of the property of Higgs bosons to couple dominantly to heavy particles, the new decay channel will quickly dominate the total decay width of the Higgs boson just above a flavor threshold. This does not mean, however, that threshold effects are unimportant; quite to the contrary, they crucially affect the total width of the Higgs boson and thus the magnitude of the signal for Higgs-boson production, which in most cases makes use of a rare decay mode of the Higgs boson ($\gamma\gamma, \tau^+ \tau^-$, etc.).

The importance of threshold effects can already be seen from the QCD corrections to the $H, P \rightarrow q\bar{q}$ decay widths, Eqs. (2.4). In the threshold region $\beta \rightarrow 0$, the corrections become

$$\Delta_H = \frac{\pi^2}{2\beta} - 1 + \frac{\pi^2}{2}\beta + O(\beta^2 \ln\beta) , \qquad (2.15a)$$

$$\Delta_P = \frac{\pi^2}{2\beta} - 3 + \frac{\pi^2}{2}\beta + O(\beta^2 \ln\beta) . \qquad (2.15b)$$

Note that the divergent parts in Δ_H and Δ_P are identical, as they should be. In both cases the QCD corrections lead to an increase of the widths; this is in sharp contrast to the opposite limit $\beta \rightarrow 1$, in which case Δ_H and Δ_P are negative.

Even though the total Higgs boson $\rightarrow q\bar{q}$ width would still be finite even for the pseudoscalar case as $\beta \rightarrow 0$, the appearance of the $1/\beta$ singularities in Eqs. (2.15) indicates that perturbation expansion breaks down and the quark picture becomes inadequate very close to threshold. Indeed it gives a wrong kinematical threshold behavior: The Higgs boson $\rightarrow q\bar{q}$ decay goes into a P-wave (S-wave) final state for the scalar (pseudoscalar), whereas the first mesonic decay modes containing the open flavor are via S wave (P wave) for the scalar (pseudoscalar); for the case $q = b$, these are $H \rightarrow B\bar{B}$ and $P \rightarrow B^*\bar{B}, B\bar{B}^*$. Since the $1/\beta$ divergences in Eqs. (2.15) are related to the formation of bound states and resonances, and these resonances decay into mesons containing the open flavor, we propose to describe the decay of H and P into this open flavor entirely by mixing with these resonance states, at least very close to threshold.

Unfortunately not even for the case $q = b$ do we have any direct experimental data on the spin-0 resonances. However, three S-wave spin-1 resonances are known, from which we can infer the masses and wave functions at the origin of two pseudoscalar resonances, $\eta(5)$ and $\eta(6)$ [see Table I(b)]. We will therefore start with a discussion of the pseudoscalar case.

We assume that Eqs. (2.1), (2.12), and (2.13) are still valid. This might be dangerous, due to the effects of mixing between different $b\bar{b}$ resonances. However, no dramatic effects of this kind seem to show up for the vector resonances, so that these equations should still be more or less correct. However, we can clearly no longer assume that the total width of $\eta(5)$ and $\eta(6)$ is dominated by the $\eta \rightarrow gg$ partial decay width; instead final states containing b-flavored mesons will be dominant. In order to estimate the resulting total widths, we introduce two simplifying assumptions. First we assume that the relevant resonances only decay into the lightest possible mesons, where we do, however, include the first spin-excited states (B^* mesons for the case $q = b$). This assumption neglects the decays of B_s's, for which evidence is reported at $\Upsilon(5)$ (Ref. 33), but these effects should more or less cancel when deriving η decays from Υ decays. To this end we write the relevant helicity amplitudes[34] as

$$\mathcal{M}(\eta \rightarrow B^*\bar{B}) = ak\delta_{\lambda 0}d^0_{0\lambda} ,$$

$$\mathcal{M}(\eta \rightarrow B^*\bar{B}^*) = ak\delta_{\lambda\bar{\lambda}}\lambda d^0_{0\lambda_f} ,$$

$$\mathcal{M}(\Upsilon \rightarrow B\bar{B}) = akd^1_{\lambda,0} , \qquad (2.16)$$

$$\mathcal{M}(\Upsilon \rightarrow B^*\bar{B}) = ak\lambda_f d^1_{\lambda_i \lambda_f} ,$$

$$\mathcal{M}(\Upsilon \rightarrow B^*\bar{B}^*) = akd^1_{\lambda_\mu \lambda_f} .$$

Here, k is the absolute value of the three-momentum of the decay products in the rest frame of the parent particle (which differs for each mode); the appearance of this factor signals that all final states are in P wave. The helicities $\lambda_i, \lambda, \bar{\lambda}$ correspond to the decaying particle and the two B mesons, respectively, and $\lambda_f = \lambda - \bar{\lambda}$. Finally, the $d^J_{\lambda\mu}$ are the well-known d functions.

Note that we assume all coupling constants a in Eqs. (2.16) to be equal; this seems reasonable since the five decay channels can be transformed into each other simply by flipping some spins, which should only have a small dynamical effect. This leads to the predictions[35] (for $m_{B^*} = 5.33$ GeV)

$$\Gamma(\Upsilon(5) \rightarrow B\bar{B}):\Gamma(\Upsilon(5) \rightarrow B^*\bar{B}, B\bar{B}^*):\Gamma(\Upsilon(5) \rightarrow B^*\bar{B}^*)$$

$$\simeq 1:3:4 , \qquad (2.17)$$

$$\Gamma(\Upsilon(6) \rightarrow B\bar{B}):\Gamma(\Upsilon(6) \rightarrow B^*\bar{B}, B\bar{B}^*):\Gamma(\Upsilon(6) \rightarrow B^*\bar{B}^*)$$

$$\simeq 1:3.5:5 ,$$

and

$$\Gamma_{\text{tot}}(\eta(5)) \simeq 0.9\Gamma_{\text{tot}}(\Upsilon(5)) ,$$

$$\Gamma_{\text{tot}}(\eta(6)) \simeq \Gamma_{\text{tot}}(\Upsilon(6)) . \qquad (2.18)$$

Had we instead assumed that all resonances only decay into the very lightest possible final states, i.e., $\Upsilon \rightarrow B\bar{B}$ and $\eta \rightarrow B^*\bar{B}, B\bar{B}^*$, we would have obtained $\Gamma_{\text{tot}}(\eta_i) \simeq 6\Gamma_{\text{tot}}(\Upsilon_i)$; the inclusion of spin-excited states is thus quite important.

As mentioned above we assume that in the threshold region the pseudoscalar P decays into open bottom only via mixing with η states; the relevant matrix elements are thus given by the last two equations of Eq. (2.16), where the coupling constant is now given by

$$|a_P|^2 = |a_5|^2|\sin\theta_5|^2 + |a_6|^2|\sin\theta_6|^2 , \qquad (2.19)$$

where the index refers to the main quantum number of the η states and θ_i is the $\eta_i - P$ mixing angle. Note that we have added the two contributions in Eq. (2.19) incoherently, since we do not have any information about the relative phase between a_5 and a_6.

The predicted $P \rightarrow$ bottom decay width according to Eq. (2.19) is shown by the long-dashed curve in Fig. 4(a); the two resonances lead to well-defined peaks above the QCD prediction for $\Gamma(P \rightarrow b\bar{b})$. On the other hand, if we only include $P \rightarrow B^*\bar{B}$ decays, which leads to much broader η resonances as discussed above, the short-dashed curve results. We show this curve not because we think it realistic but because it shows a curious phenomenon that will be important for H decays: Its maximum is only a little above the QCD prediction for $P \rightarrow b\bar{b}$; indeed, if the resonances were even broader, the curve would smoothly approach the QCD prediction from below.

Of course, the assumption that P decays into bottom only via mixing with η states clearly becomes inadequate high above the threshold, where the QCD prediction for $P \rightarrow b\bar{b}$ should be quite reliable. We therefore have to find a way to interpolate between the QCD region and the resonance region. We choose the following interpolation:

$$\Gamma(P \rightarrow \text{bottom})$$

$$= \Gamma(P \rightarrow B \text{ mesons})$$

$$+ \Gamma_{\text{QCD}}(P \rightarrow b\bar{b})\left\{1 - \exp\left[-\left[\frac{x}{a}\right]^b\right]\right\} , \qquad (2.20)$$

with $x = 2k_{B^*}/m_P$. This is shown by the solid curve in Fig. 4(a), where we choose $b = 5$ in order to reproduce the behavior right at threshold, and $a = 0.373$, which implies that the integrals over the solid and upper dotted curves are equal, in the spirit of QCD sum rules.

Unfortunately there are no experimental data on P-wave $b\bar{b}$ resonances available; we can thus not directly compute the mixing between H and χ resonances. Recall, however, that these scalar resonances decay into S-wave $B\bar{B}$ and $B^*\bar{B}^*$ states; we can expect them to be very broad. As indicated by the short-dashed curve in Fig. 4(a) and the discussion above, the mixing-induced $H \rightarrow$ bottom width can therefore be expected to go more

or less smoothly into the QCD prediction for $H \rightarrow b\bar{b}$. It is interesting to note at this point that the inclusion of QCD corrections to $\Gamma(P \rightarrow b\bar{b})$ makes the transition (for very broad resonances) much smoother. Such a behavior can be adequately described by Eq. (2.20) if we drop the first term altogether and instead choose a somewhat smaller value for b. Note that this results in a threshold behavior $\sim k^b$; since H decays into an S wave, it seems reasonable to choose b two units smaller here than what one would need for a very broad P-wave resonance. For the solid curve in Fig. 4(b) we thus choose $b = 1.6$, $a = 0.26$. We also show a curve for $b = 1$, which can be viewed as a parametrization of an interpolation between the true kinematical threshold and the $H \rightarrow b\bar{b}$ width; in

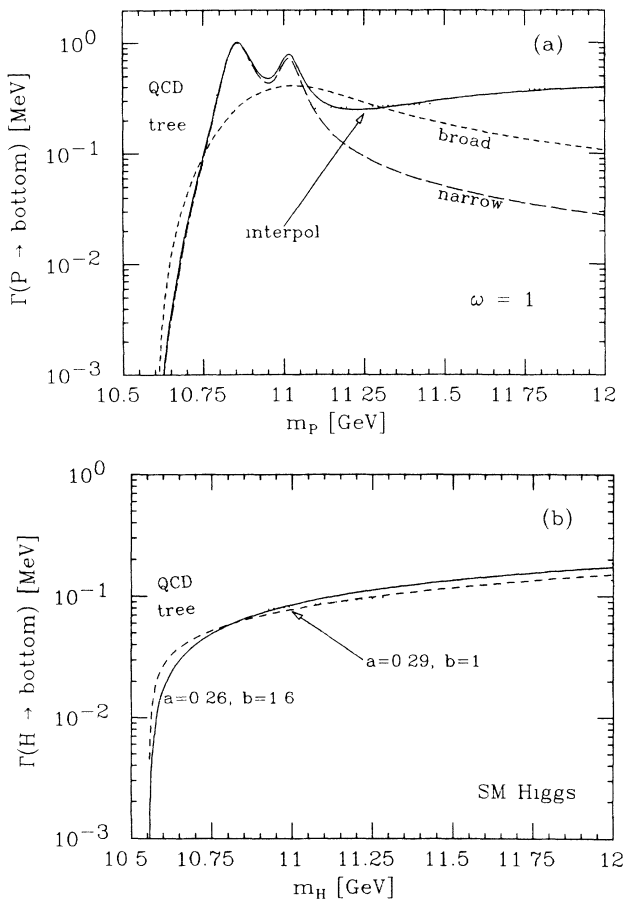this case, a is chosen to give an optimally smooth interpolation in the pseudoscalar case (for very broad resonances) with fixed $b = 3$. This latter choice leads to a sizable suppression of the $H \rightarrow$ bottom width compared to the QCD prediction even for $m_H \simeq 12$ GeV, i.e., almost 1.5 GeV above threshold. Data on the total hadronic cross section in e^+e^- annihilation seem to be very close[22] to the perturbative QCD prediction already at $\sqrt{s} = 12$ GeV, which indicates that the solid curve is probably closer to the correct answer. Of course, we cannot exclude the possibility of the existence of a χ resonance with a width of "only" a few hundred MeV, which should give rise to a sizable bump in the $H \rightarrow$ bottom width, similar to the short-dashed curve in Fig. 4(a).

This completes our discussion of Higgs boson $\rightarrow$ bottom decays near threshold. We are now in a position to compute branching ratios for the various Higgs-boson decays in the whole threshold region.

C. Summary of Higgs-boson decays around the $b\bar{b}$ threshold

In Figs. 5(a) and 5(b) we summarize the various branching ratios for a scalar and pseudoscalar Higgs boson with mass around 10 GeV. In both cases we have chosen all Yukawa coupling to have standard strength. This corresponds to $\omega = 1$ in the pseudoscalar case and $m_P^2 \gg m_Z^2$, $1.10 \leq \omega \leq 1.14$ in the scalar case within the minimal supersymmetric model. [Of course, Fig. 5(a) is also valid for the SM Higgs boson.] The solid and dashed curves include QCD corrections and mixing effects, whereas the dotted curves show the τ-pair branching ratios for $\alpha_s = 0$ and without mixing.

We again see that the region where mixing is important is much larger in the pseudoscalar case, due to both the larger number of pseudoscalar bound states and the larger value of δm^2 [cf. Eqs. (2.1)]. However, in both cases we see that threshold effects in the wider sense are quite important even for the Higgs boson$\rightarrow \tau^+ \tau^-$ branching ratio, which is affected almost only by the change of the total decay width of the Higgs boson, over a region of several GeV; the effects are, however, quite different in the cases.

In case of a scalar Higgs boson with mass around 9 GeV the inclusion of QCD corrections increases the τ-pair branching ratio; the reduction of the Higgs boson$\rightarrow c\bar{c}$ decay width[2] more than compensates the contribution from Higgs boson $\rightarrow gg$ to the total width of the Higgs boson. For a pseudoscalar Higgs boson of the same mass, the gluonic decay width is already quite large, reducing the τ pair branching ratio by about 50%. As the Higgs-boson mass approaches the mass of the first $b\bar{b}$ bound state the gluonic decay width increases rapidly; in both cases there is a region where the branching ratio for Higgs boson$\rightarrow gg$ is close to 100%, leading to a situation where the Higgs boson looks like a $b\bar{b}$ bound state. However, a scalar Higgs boson can be "hidden" in this fashion only if it lies within 10 MeV or so of one of the χ states. As discussed in Sec. II A, this is probably already excluded experimentally. In contrast, the regions where $B(P \rightarrow gg) > 50\%$ add up to about 350 MeV; the possibil-

FIG. 4. Decay widths of P (a) and H (b) into open bottom just above the physical threshold. The two dashed curves in (a) differ by the assumed total decay widths of the two pseudoscalar resonances $\eta(5)$ and $\eta(6)$. "Narrow" corresponds to the values derived from our model including all possible combinations of B and B^* mesons in Υ and η decays for these resonances as described in the text, while the curve labeled "broad" is valid if only the lightest final states contribute. The dotted lines in both figures show quark-model predictions for $H, P \rightarrow b\bar{b}$ with and without QCD corrections. The solid curve in (a) is an interpolation between the long-dashed and upper dotted curves as discussed in the text, while the solid and dashed curve in (b) show a similar interpolating function (2.20) without the first term in the scalar case with different values of the parameters a and b.

ity that a pseudoscalar Higgs boson might not look like a Higgs boson at all should therefore be taken seriously.

The behavior of the τ pair branching ratio in the region where the Higgs bosons can decay into open bottom also differs in the two cases. Just above threshold the modified threshold function (2.20) reduces the $H\rightarrow$ bottom decay width compared to the tree-level Higgs boson$\rightarrow b\bar{b}$ decay width, but for somewhat higher Higgs-boson masses the positive QCD corrections become more important, increasing the total decay width of the scalar Higgs bosons. In contrast, the two narrow pseudoscalar resonances enhance the $P\rightarrow$ bottom decay width directly after the threshold, whereas QCD enhancement is again visible for somewhat larger m_P; the net effect is that $B(P\rightarrow\tau^+\tau^-)$ is almost always suppressed compared to the naive-quark-model calculation. Note, however, that the P-wave suppression of $H\rightarrow b\bar{b}$ is still operative for $m_H = 12$ GeV, leading to a τ pair branching ratio of almost 10%, almost twice as high as in the pseudoscalar case.
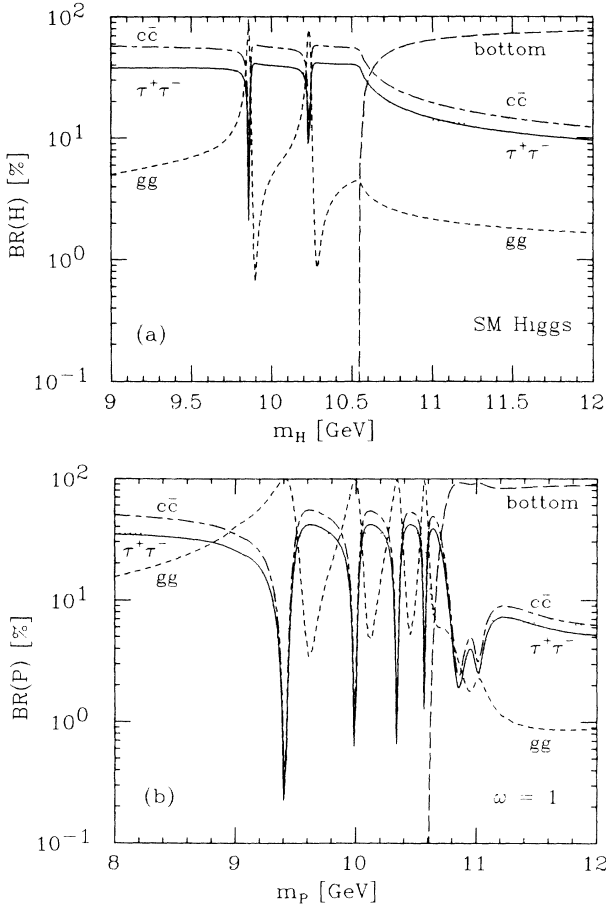

FIG. 5. A summary of branching ratios for various decay modes of the scalar (a) and pseudoscalar (b) Higgs boson around the $b\bar{b}$ threshold. All Yukawa couplings are assumed to have the SM strength, and the b-quark contribution has been included in the $H,P\rightarrow gg$ loop. One-loop QCD corrections have been taken into account for the $c\bar{c}$ mode, while the open bottom mode has been calculated using Eq. (2.20) as shown in Fig. 4. For comparison the dotted curves show the branching ratios into τ pairs with $\alpha_s = 0$ and no mixing.

How do all these branching ratios change if $\omega > 1$? First of all, the $c\bar{c}$ mode is suppressed compared to the $\tau^+\tau^-$ and $b\bar{b}$ modes; in the pseudoscalar case, $\Gamma(P\rightarrow\tau^+\tau^-)/\Gamma(P\rightarrow c\bar{c})\sim\omega^4$. The $c\bar{c}$ mode thus becomes quickly unimportant. Second, the region where the Higgs boson is "hidden" by mixing with a bound state grows somewhat; however, it approaches a constant as the $c\bar{c}$ mode becomes unimportant, since for larger ω both the width of the unmixed Higgs boson and the mixing contribution to Higgs boson $\rightarrow gg$ grow like ω^2.

In the (theoretically disfavored[36]) case $\omega < 1$ the $c\bar{c}$ mode becomes more important, overwhelming even the Higgs boson$\rightarrow$bottom decay mode if $\omega < \frac{1}{3}$; furthermore, the region where mixing is important shrinks.

III. HIGGS-BOSON PRODUCTION VIA TWO-GLUON FUSION

We have seen in Sec. II that the most dramatic effect of mixing between Higgs bosons and heavy $q\bar{q}$ bound states is the possibly large enhancement of the Higgs boson$\rightarrow gg$ decay width. Of course this also implies that the $gg\rightarrow$ Higgs-boson cross section is enhanced by the same factor. In this section we investigate whether this might allow for the detection of Higgs bosons with masses around 10 GeV in hadronic collisions.

The only Higgs-boson decay mode with a sizable branching ratio which one might be able to detect in a hadronic environment is the Higgs boson$\rightarrow\tau^+\tau^-$ mode. Here we will assume that one can indeed trigger on events in which the two τ leptons are the only particles with a sizable transverse momentum. Under this condition the background is given by the Drell-Yan production of τ pairs. It is therefore advantageous to consider pp rather than $p\bar{p}$ collisions, since in the former case the background cross section contains at least one sea quark. Furthermore, since we are interested in fairly light Higgs bosons, the center-of-mass energy $\sqrt{s}$ need not be very high. We will therefore focus on fixed target experiments at the Fermilab Tevatron ($\sqrt{s} = 43$ GeV) and the Serpukhov UNK ($\sqrt{s} = 75$ GeV).

The most obvious "signal" would be a peak in the τ-pair invariant-mass spectrum. Unfortunately this is not directly measurable, since τ decay products always contain invisible neutrinos. However, the produced τ leptons will be quite fast; it should therefore be possible to reconstruct the angle and thus the rapidity of τ leptons with reasonable precision. One might then hope to find different rapidity distributions for signal and background, due to the different initial states and the different kinematical situation.

After integration over the transverse momentum the rapidity distribution of the τ leptons that result from Higgs-boson decay is given by

$$\frac{d^2\sigma(pp\rightarrow AX\rightarrow\tau^+\tau^- X)}{dy_1 dy_2}$$
$$= \frac{\pi^2\Gamma(A\rightarrow gg)B(A\rightarrow\tau^+\tau^-)}{32s\beta m_A\cosh^2\frac{1}{2}(y_1-y_2)}g(x_1)g(x_2), \quad (3.1)$$

where

$$x_1^2 = \tau e^{y_1 + y_2}, \quad x_2^2 = \tau e^{-(y_1 + y_2)}, \tag{3.2a}$$

with

$$\tau = m_A^2 / s \tag{3.2b}$$

and

$$\beta = \left[1 - \frac{4m_\tau^2}{m_A^2} \right]^{1/2}. \tag{3.2c}$$

y_1 and y_2 are the τ^+ and τ^- rapidities in the pp center-of-mass frame; the corresponding quantities in the laboratory frame can be obtained by adding $\ln(\sqrt{s}/m_p)$. The symbol A in Eqs. (3.1) and (3.2) stands for H and P, and $g(x)$ is the gluon density inside the proton, evaluated at $Q^2 = m_A^2$. The hyperbolic function in the denominator results from integrating the transverse momentum of the τ leptons over $\delta(x_1 x_2 s - m_A^2)$. Note that it is minimal for $y_1 = y_2$, which corresponds to maximal transverse momentum for fixed τ-pair invariant mass.

The Drell-Yan τ pair background is given by

$$\frac{d^3\sigma(pp \to \tau^+\tau^- X)}{dp_T^2 dy_1 dy_2}$$

$$= \sum_{\text{flavors}} \frac{\pi e_q^2 \alpha^2}{3s^2\tau} \left[1 + \frac{4m_\tau^2}{s\tau} + \tanh^2\frac{y_1 - y_2}{2} \right]$$

$$\times [q(x_1)\bar{q}(x_2) + \bar{q}(x_1)q(x_2)]. \tag{3.3}$$

Here x_1 and x_2 are still given by Eq. (3.2) except that

$$\tau = \frac{4(p_T^2 + m_T^2)}{s}\cosh^2\frac{y_1 - y_2}{2}$$

is no longer fixed, and p_T^2 is the squared transverse momentum of either τ lepton. Note that, since we are considering pp collisions, $\bar{q}(x)$ comes from sea quarks only; at the moderate values of $\sqrt{s}$ of interest for us $q(x)$ is then dominated by the contribution from valence quarks. Of course, in order to compare the background (3.3) with the signal (3.1), we have to (numerically) integrate Eq. (3.3) over the allowed range of p_T^2.

Two effects dominate the rapidity distribution of the background. First, the s-channel photon propagator favors small values of $\hat{s}$, i.e., small values of $|y_1 - y_2|$; this unfortunately mimics the effect of the Jacobian factor in the signal cross section (3.1). Second, the fact that valence-quark distributions extend to much larger values of x than sea-quark distributions favors situations where x_1 and x_2 are quite different. However, that does not necessarily imply that y_1 and y_2 are also different; in fact this effect favors situations where both rapidities have the same sign. In contrast, the gluon flux factor in the signal cross section (3.1) is maximal if $x_1 = x_2$, i.e., $y_1 = -y_2$.

In Fig. 6 we therefore show the rapidity distribution of signal and background for fixed $y_1 = +1$ at $\sqrt{s} = 43$ GeV (6a) and 75 GeV (6b). The signal has been computed for $m_P = 9.3$ GeV, $\omega = 5$. We see that for this combination of parameters the signal clearly dominates the background if y_2 is sufficiently negative. Note that the signal includes contributions not only from H and P, but also from the η

and χ_0 states; these latter contributions are sizable if mixing is large. We also see that mixing increases the signal cross section by almost one order of magnitude. Indeed from Figs. 3 one can read off that the total cross section for H and P production is enhanced by an even larger factor; however, for the given choice of parameters the total P decay width is already dominated by its decay into two gluons, and the branching ratio into τ pairs is suppressed [see Fig. 5(b)].

In Fig. 6 we also show the effect of imposing a mild cut on the τ pair invariant mass $m_{\tau^+\tau^-} > 6$ GeV. Since this cut only necessitates the measurement of the invariant mass with about 30% precision, something like it might actually be implementable experimentally. If so, the signal becomes dominant for all negative y_2 at the Tevatron,
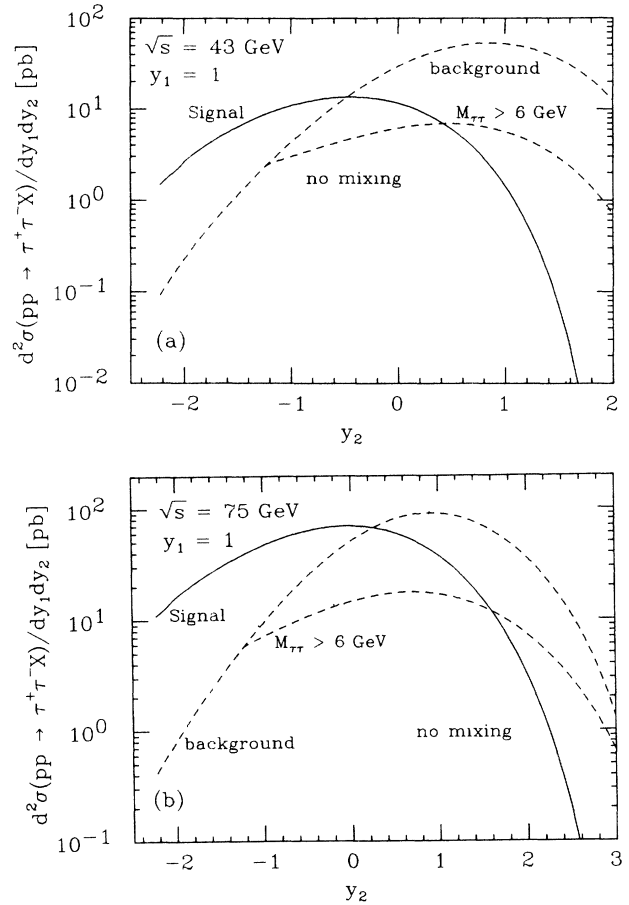

FIG. 6. Differential cross sections for $pp \to \tau^+\tau^- X$ at (a) $\sqrt{s} = 43$ GeV and (b) $\sqrt{s} = 75$ GeV, corresponding to Tevatron and UNK fixed-target experiment, respectively. The signal has been computed for $m_P = 9.3$ GeV, $\omega = 5$. The solid curve contains contributions from the physical-Higgs-boson-like particles as well as the χ_0- and η-like states, whereas the dotted curves show the prediction for unmixed H and P states. b quarks have been included in the $gg \to H, P$ loops everywhere. The cross sections are integrated over the transverse momentum of the τ leptons, and all rapidities are in the pp center-of-mass frame. The background (dotted curves) has been estimated from lowest-order Drell-Yan production; for the lower dashed curves the cut $m_{\tau\tau} > 6$ GeV has been applied.

and even dominates the integrated cross section at $y_1 = 1$ at the UNK accelerator. The reason for the better signal-to-background ratio at the UNK is that even at $\sqrt{s} = 75$ GeV the background is dominated by valence quarks, whose flux grows more slowly with decreasing x than the gluon flux of the signal. However, all QCD cross sections also rise strongly with energy; at some point instrumental backgrounds like jets faking τ leptons, might become a problem. On the other hand, even at the Tevatron the event rates should be high enough to allow one to apply quite stringent experimental cuts on the actually observed particles in order to get rid of such nonphysics background.

From Fig. 6 we thus conclude that if the total signal cross section is as large as for $m_P = 9.3$ GeV, $\omega = 5$, i.e., 100 pb at $\sqrt{s} = 43$ GeV, the signal should in principle be observable, and that even half that value (50 pb) might be enough. In Fig. 7 we therefore show lines of constant $\sigma(pp \to H, P, \eta, \chi_0 \to \tau^+ \tau^- X)$ in the $m_P - \omega$ plane at $\sqrt{s} = 43$ GeV, for $\sigma = 50$ and 100 pb (solid lines). In general larger values of ω correspond to a larger cross section. For small mixing, increasing ω increases mixing and thus the cross sections for H, P production, whereas for large mixing, an increase of ω increases the branching ratio for the decay of the mixed states into $\tau^+ \tau^-$. The four subthreshold η_b bound states therefore clearly manifest themselves as minima, whereas the negative interference in the $P \to gg$ matrix element that occurs if m_P is just above the mass of one of the bound states results in well-defined maxima. The situation is somewhat more complicated for the contributions from H and the χ states, since m_H depends on both m_P and ω; the $\chi_0(9860)$ thus produces minima at $m_P = 10.5$ GeV for $\sigma = 50$ pb, corresponding to $\omega \simeq 5.5$, and at $m_P = 10.35$ GeV for $\sigma = 100$ pb, corresponding to $\omega \simeq 6$, the latter one almost at the same point as the minimum corresponding to $\eta(10\,340)$. In general we can conclude that if $\omega \gtrsim 5$, the $\tau^+ \tau^-$ signal might well be observable at the Tevatron if
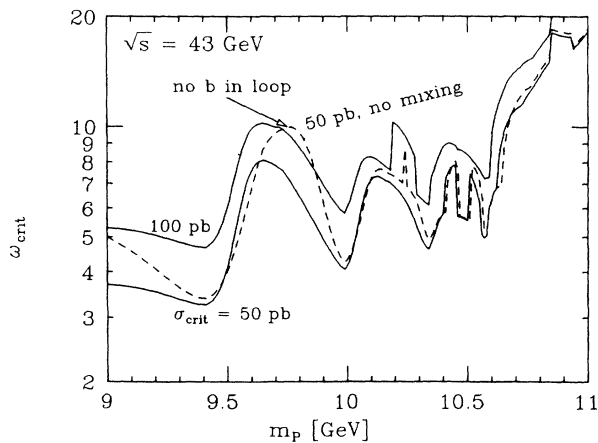
$m_P \lesssim 10.5$ GeV. In this context it might be interesting to note that there have recently been attempts in the literature[37] to construct models with $\omega \simeq m_t / m_b \gtrsim 10$. This is possible even within minimal supergravity models[36] if $m_t \gtrsim 55$ GeV, which now seems favored by $p\bar{p}$ collider data;[38] furthermore, certain superstring models[39] tend to give similar Yukawa couplings for b and t quarks. If indeed $\omega \sim 10$, Fig. 7 seems to indicate that a Higgs-boson signal should always be detectable at the Tevatron if only $m_P \lesssim 10.5$ GeV; however, we have to keep in mind that our method of extracting a τ signal only works for highly relativistic τ leptons, and thus clearly breaks down for too light Higgs bosons, which might, alas, already be ruled out[8] experimentally by the nonobservation[40] of Wilczek decay of Υ mesons.

It has been suggested[41] that a Higgs boson produced with a large transverse momentum, decaying to a τ pair, may provide a possible signature at collider energies. The responsible process, $gg \to$ Higgs boson $+g$, may also be enhanced by the mixing with a quarkonium. The effect, however, is weaker than what we have discussed since the process $gg \to \eta, \chi_0 + g$ has a steeper p_T dependence[42] than the quark-loop induced process. Moreover, the cross section at large p_T should be very small at fixed-target energies.

Finally it should be mentioned that for $m_P \lesssim 11$ GeV and $\omega \gtrsim 3$ the $e^+ e^- \to HP$ cross section is[8] around 1 pb at TRISTAN energies, $\sqrt{s} \sim 60$ GeV. However, as discussed in the previous section, if mixing effects are big enough, the Higgs bosons might not look like Higgs bosons at all and could thus be hard to detect at TRISTAN. Second, one can construct (nonminimal) models[43] with small m_p and large ω which still have a small or vanishing $e^+ e^- \to HP$ cross section. For this reason, even if no HP signal will be found at TRISTAN, an independent check from a completely different type of experiment will still be useful.

IV. SUMMARY AND CONCLUSIONS

In this paper we tried to give a comprehensive treatment of the production and decay of Higgs bosons with mass close to a heavy $q\bar{q}$ threshold. Using the minimal supersymmetric model as a guideline, we discussed both scalar and pseudoscalar Higgs bosons. As a practical application of possibly immediate experimental relevance we studied the properties of Higgs bosons with mass around 10 GeV, i.e., near the bottom threshold, in some detail.

Perhaps somewhat surprisingly we found threshold effects (defined as deviations from the simple tree-level Higgs boson $\to q\bar{q}$ decay model) to be most dramatic just below the open flavor threshold. Here mixing between Higgs bosons and $q\bar{q}$ bound states can result in large decay widths and even branching ratios for the Higgs boson $\to gg$ decay mode, leading in the most extreme case to physical particles which hardly bear any resemblance to "usual" Higgs bosons. While this might make it harder to detect Higgs bosons at $e^+ e^-$ colliders, it might allow for their detection at proton fixed-target experiments at the Tevatron or UNK, as discussed in Sec. III. Since

FIG. 7. Lines of constant $\sigma(pp \to H_M, P_M, \chi_M, \eta_M \to \tau^+ \tau^- X)$ at $\sqrt{s} = 43$ GeV. For the upper (lower) solid line, mixing has been included and $\sigma_{crit} \equiv \sigma(\omega_{crit}) = 100$ pb (50 pb). For the dashed curve, $\sigma_{crit} = 50$ pb without inclusion of b-loop contributions to $b\bar{b} \to H, P$. Finally, on the dotted curve $\sigma_{crit} = 50$ pb if all mixing effects are neglected.

the main ingredients of the calculation of these mixing effects are the nonrelativistic potential model, which describes the known $b\bar{b}$ bound states quite successfully, and QCD, we feel that our results are quite reliable in this region; as discussed in Sec. II A, the main theoretical uncertainty is related to the question how the Higgs boson$\rightarrow q\bar{q}\rightarrow gg$ loop diagram should be treated near the $q\bar{q}$ threshold.

Similarly, our results should be very reliable once we surpass the physical threshold (in our case $2m_B$) by more than 1 GeV or so. In this region, one-loop QCD corrections, which diverge as the Higgs-boson mass approaches $2m_q$, are still quite important, but not so big as to be totally unreliable. Note that they are positive, whereas in the limit of large m_H/m_q they are negative (and also large).

It is within 1 GeV or so above the physical open-flavor threshold where our results are perhaps least reliable. We started from the assumption that in this region Higgs bosons decay into the new open flavor only via mixing with $q\bar{q}$ resonance states in the spirit of the vector-meson-dominance model; some of the ingredients of our model, such as the use of a nonrelativistic potential model and the universal coupling for all channels, may be oversimplification. We were thus quite surprised when we found that this crude description naturally led to a smooth transition to the region where the QCD-corrected Higgs boson$\rightarrow q\bar{q}$ decay width should be reliable. Especially the fact that inclusion of the QCD corrections proved to be crucial for the smoothness of this transition (at least in the limit of very broad resonances) seems to indicate that our model, simplistic as it may be, does contain some of the real dynamics in the threshold region.

In this paper we have concentrated on the mixing of a neutral Higgs boson with quarkonium states. A similar effect occurs for a charged Higgs boson H^+ if its mass lies near the mass of $(t\bar{b})$ mesons. [Mixing with $(t\bar{s})$ or $(t\bar{d})$ states will be suppressed by small Kobayashi-Maskawa mixings and smaller decay constants.] Since both constituents of a $(t\bar{b})$ meson are heavy, the nonrelativistic potential-model picture is a good approximation, and the formalism of this paper can be applied without major modification. The main differences are the absence of the gg decay mode and the importance of the weak decay modes instead.

Finally one might ask how big the "probability" might be that threshold effects can be felt, i.e, in what fraction of parameter space the effects discussed in this paper are important. The answer may be surprisingly large. The lower border of the threshold region can be defined as the point where $P\rightarrow gg$ decays become affected by P-η mixing, i.e., around 8–8.5 GeV for the case of $q=b$, whereas as upper border one might use the point where QCD corrections turn from positive to negative, i.e., $m_H\simeq 4.3m_b$ or $m_P\simeq 3.7m_b$. The upper boundary obviously scales linearly with m_q, and this should also approximately hold for the lower boundary. In this broad sense threshold effects are thus important over a region of size more than $2m_q$. Mixing effects can be important in a region of size 0.4–$0.5m_q$ for the pseudoscalar case and perhaps 0.1–$0.2m_q$ for the scalar case.[44] We are thus led

to conclude that any comprehensive strategy to search for Higgs bosons has to take these effects into account as far as quantitative predictions are concerned, and that even the possibility of Higgs signals and cross sections being qualitatively different than predicted by simple tree-level calculations should be taken seriously.

Note added in proof. After the submission of the paper, we were informed that L. Bergström, [Z. Phys. C **20**, 135 (1983)] calculated radiative corrections to $P\rightarrow f\bar{f}$ in the limiting case $m_P\gg m_f$. His result agrees with our Eq. (2.4b) if we take the limit $\beta\rightarrow 1$. We are grateful to L. Bergström for correspondence.

APPENDIX A: NEUTRAL HIGGS SECTOR IN THE MINIMAL MODEL

In this appendix we briefly review some relevant details of the minimal supersymmetric Higgs model. We refer the reader to Refs. 45 and 13 for more details.

Before symmetry breaking the Higgs sector consists of a $Y=-\frac{1}{2}$ doublet H and a $Y=+\frac{1}{2}$ doublet $\bar{H}$. After symmetry breaking the physical-Higgs-boson spectrum contains one charged Higgs $H^\pm$, one neutral pseudoscalar P, and two neutral scalars H,H', with H being the lighter state. All masses and mixing angles can be expressed in terms of m_P and $\omega\equiv\langle\bar{H}^0\rangle/\langle H^0\rangle$, where all existing models[36] predict $\omega\gtrsim 1$. In particular the mass of the light scalar is given by

$$m_H^2=\tfrac{1}{2}[m_P^2+m_Z^2-\sqrt{(m_P^2+m_Z^2)^2-4m_P^2m_Z^2\cos^2 2\beta}]\ ,$$

$$(A1)$$

where $\tan\beta=\omega$. In the limit $m_P^2\ll m_Z^2$ this becomes

$$m_H\simeq m_P|\cos 2\beta|=m_P\left|\frac{\omega^2-1}{\omega^2+1}\right|\ ,\qquad (A2)$$

as mentioned in the beginning of Sec. II.

The couplings of H and P to quarks and leptons f can be written in the form

$$\mathcal{L}_{\text{Yukawa}}=\sum_f(\sqrt{2}\,G_F)^{1/2}m_f(C_{Hf\bar{f}}Hf\bar{f}+iC_{Pf\bar{f}}P\bar{f}\gamma_5 f)\ ,$$

$$(A3)$$

where

$$C_{Hu\bar{u}}=-\frac{\cos\alpha}{\sin\beta},\quad C_{Hd\bar{d}}=C_{Hl\bar{l}}=\frac{\sin\alpha}{\cos\beta}\ ,$$

$$C_{Pu\bar{u}}=\cot\beta,\quad C_{Pd\bar{d}}=C_{Pl\bar{l}}=\tan\beta\ .$$

$$(A4)$$

Here α is the angle describing the mixing between the neutral Higgs scalars. It is given by

$$\tan 2\alpha = \frac{m_P^2 + m_Z^2}{m_P^2 - m_Z^2} \tan 2\beta , \tag{A5}$$

with the additional constraint $-\frac{1}{4}\pi \le \alpha \le 0$ if $m_P < m_Z$, $\omega < 1$ or $m_P > m_Z, \omega > 1$, while $-\frac{1}{2}\pi \le \alpha \le -\frac{1}{4}\pi$ otherwise. Since one can always choose $0 \le \beta \le \frac{1}{2}\pi$, this implies that $C_{Hu\bar{u}}$ and $C_{Hd\bar{d}}$ have the same sign and are indeed negative. Note finally that for $\omega^2 \gg 1$, scalar and pseudoscalar couplings become equal in strength.

In the (nonsupersymmetric) minimal standard model, the Yukawa couplings are given by Eq. (A3) with

$$C_{Hu\bar{u}} = C_{Hd\bar{d}} = C_{Hl\bar{l}} = -1 \tag{A6}$$

and without P.

APPENDIX B: PARTICLE-MIXING FORMALISM

Here we give a brief description of mixing between different particles for the case of finite decay widths, following closely the discussion of Ref. 9.

We start with the simple case of one Higgs boson H mixing with one bound state χ. The mass matrix is then

$$\mathcal{M}^2 = \begin{array}{c} \\ H \\ \chi \end{array} \begin{pmatrix} m_H^2 - im_H\Gamma_H & \delta m_H^2 \\ \delta m_H^2 & m_\chi^2 - im_\chi\Gamma_\chi \end{pmatrix} , \tag{B1}$$

where δm_H^2 is given in Eq. (2.1a). It is useful to introduce a complex quantity Δ^2:

$$\Delta^2 = [\frac{1}{4}(m_H^2 - m_\chi^2 - im_H\Gamma_H + im_\chi\Gamma_\chi)^2 + (\delta m_H^2)^2]^{1/2} . \tag{B2}$$

The masses and decay widths of the two physical (mixed) eigenstates are then found to be

$$m_{1,2}^2 - im_{1,2}\Gamma_{1,2} = \frac{1}{2}(m_H^2 + m_\chi^2 - im_H\Gamma_H - im_\chi\Gamma_\chi) \pm \Delta^2 . \tag{B3}$$

We thus see that for $m_H > m_\chi$, the "Higgs-boson-like" state H_M is to be identified with state 1, whereas for $m_H < m_\chi$ it is state 2. In cases of interest to us we find the mass shift due to Eq. (B3) to be negligibly small, whereas the effect on the total widths can be sizable, as

discussed in Sec. II.

The angle between H_M and H is in general complex:

$$H_M = \frac{1}{\sqrt{N}}(H\cos\theta + \chi\sin\theta) ,$$

$$N = |\sin\theta|^2 + |\cos\theta|^2 , \tag{B4}$$

with

$$\sin\theta = \frac{\delta m_H^2}{[(\delta m_H^2)^2 + X^2]^{1/2}} ,$$

$$\cos\theta = \frac{X}{[(\delta m_H^2)^2 + X^2]^{1/2}} , \tag{B5}$$

where

$$X = m_{H_M}^2 - m_\chi^2 - im_{H_M}\Gamma_{H_M} + im_\chi\Gamma_\chi .$$

Note that X depends on the mass and width of the physical, mixed Higgs-boson state, but the unmixed χ state. Since H_M is either state 1 or state 2, this explains the change of sign of the real part of $\sin\theta\cos\theta$ shown in Fig. 2. For small angle, the mixing angle can be approximated as

$$\theta \simeq \tan\theta \simeq \frac{\delta m_H^2}{m_H^2 - m_\chi^2 - im_H\Gamma_H + im_\chi\Gamma_\chi} . \tag{B6}$$

In the case of more than one bound state χ_i, it is for our purposes always sufficient to use the approximate formula (B6) for all but one bound state, namely, the state χ_C closest in mass to m_H. We can then write

$$H_M = \frac{1}{\sqrt{N}}(H\cos\theta_C + \chi_C\sin\theta_C) + \frac{1}{\sqrt{N}}\cos\theta_C \sum_{i \ne C} \theta_i\chi_i , \tag{B7}$$

where the coefficient in front of the sum comes from the fact that the state that mixes only weakly is given by the first term in parentheses in Eq. (B7); however, for practical purposes this coefficient can be set to one, since for large H-χ_C mixing, i.e., $|\cos\theta_C|$ appreciably away from one, the contribution from χ_C swamps those from the other χ states.

[1] For reviews, see, e.g., G. Altarelli, in *Proceedings of the Workshop on Physics at Future Accelerators*, La Thuile and Geneva, 1987, edited by J. H. Mulvey (CERN Report No. 87-07, Geneva, 1987), Vol. I, p. 36; V. Barger, in *Proceedings of the XXIV International Conference on High Energy Physics*, Munich, West Germany, 1988, edited by R. Kotthaus and J. H. Kühn (Springer, Berlin, 1989), p. 1265; R. N. Cahn, Rep. Prog. Phys. **52**, 389 (1989).

[2] E. Braaten and J. P. Leveille, Phys. Rev. D **22**, 715 (1980). See also N. Sakai, *ibid.* **22**, 2220 (1980); T. Inami and T. Kubota, Nucl. Phys. **B179**, 171 (1981).

[3] J. Schwinger, *Particles, Sources, and Fields* (Addison-Wesley, Reading, MA, 1973), Vol. II, Chap. 5–4. See also Sec. 7.3 of V. A. Novikov *et al.*, Phys. Rep. **41C**, 1 (1978).

[4] For reviews, see, e.g., C. Quigg and J. L. Rosner, Phys. Rep. **56**, 167 (1979); W. Kwong, J. L. Rosner, and C. Quigg, Annu. Rev. Nucl. Part. Sci. **37**, 325 (1987).

[5] J. Ellis, M. K. Gaillard, D. V. Nanopoulos, and C. T. Sachrajda, Phys. Lett. **83B**, 339 (1979).

[6] For reviews, see H. P. Nilles, Phys. Rep. **110**, 1 (1984); P. Nath, R. Arnowitt, and A. H. Chamseddine, *Applied N=1 Supergravity* (World Scientific, Singapore, 1984).

[7] H. Baer *et al.*, in *Physics at LEP*, LEP Jamboree, Geneva, Switzerland, 1985, edited by J. Ellis and R. D. Peccei (CERN Report No. 86-02, Geneva, 1986), Vol. 2, p. 297.

[8] M. Drees and K. Hikasa, Phys. Rev. D **40**, 47 (1989).

[9] P. J. Franzini and F. J. Gilman, Phys. Rev. D **32**, 237 (1985). See also L. J. Hall, S. F. King, and S. R. Sharpe, Nucl. Phys.

B260, 510 (1985); S. Güsken, J. H. Kühn, and P. M. Zerwas, *ibid.* B262, 393 (1985).

[10] In order to get a finite result for the QCD corrections (2.4), the $Aq\bar{q}$ vertex has to be renormalized; the appropriate counterterm is uniquely fixed by the quark-mass and wave-function counterterms for both H and P. We have calculated the full $O(\alpha_s)$ corrections and our results for H agree with Ref. 2. Closely related calculations of the scalar and pseudoscalar operator two-point functions were done in the context of QCD sum rules; the adopted renormalization conditions in these calculations are not necessarily suitable for the case of Higgs couplings. The original results for the scalar and pseudoscalar in L. J. Reinders, H. R. Rubinstein, and S. Yazaki, Nucl. Phys. B186, 109 (1981), in fact do not agree with ours and Ref. 2. The pseudoscalar result in Ref. 11, however, agrees with ours.

[11] L. J. Reinders, H. Rubinstein, and S. Yazaki, Phys. Rep. 127, 1 (1985).

[12] Inami and Kubota (Ref. 2).

[13] J. F. Gunion and H. E. Haber, Nucl. Phys. B278, 449 (1986).

[14] In Eq. (2.6) summation over gluon color has been performed.

[15] The Higgs-squark couplings relevant to Higgs boson→gg decay consists of two terms: a Yukawa-type (F-term) coupling being proportional to m_q^2/m_W and a D-term coupling proportional to m_W. If the four squark states of one generation are mass degenerate, the possibly important D term coupling cancels exactly, leaving the Yukawa coupling contribution. In the case $\omega \gg 1$, the D-term mass splitting of squarks may be large. The Higgs-squark D-term coupling, however, has a mixing factor which vanishes for $m_{\tilde{P}}^2 \ll m_Z^2$. Thus the squark contribution to the Higgs boson→gg loop is always small for the Higgs-boson mass region of our interest here.

[16] UA1 Collaboration, C. Albajar *et al.*, Phys. Lett. B 198, 261 (1987); CDF Collaboration, F. Abe *et al.*, Phys. Rev. Lett. 62, 1825 (1989).

[17] There is no agreement in the literature concerning the sign of the imaginary part of $I(x)$. We double-checked the sign in Eq. (2.8) with unitarity. Our sign agrees with that in A. I. Vainshtein, M. B. Voloshin, V. I. Zakharov, and M. A. Shifman, Yad. Fiz. 30, 1368 (1979) [Sov. J. Nucl. Phys. 30, 711 (1979)] but disagrees with that in, e.g., R. N. Cahn and S. Dawson, Phys. Lett. 136B, 196 (1984); E. Eichten, I. Hinchliffe, K. Lane, and C. Quigg, Rev. Mod. Phys. 56, 579 (1984), and Ref. 13. Note that the sign of $I(x)$ has no effect on the previous results, with the notable exception of K. J. F. Gaemers and F. Hoogeveen, Phys. Lett. 146B, 347 (1984), in which the correct sign is used. The sign is important for our study because the mixing angle is complex.

[18] J. H. Kühn and P. M. Zerwas, Phys. Rep. 167, 321 (1988).

[19] V. Barger *et al.*, Phys. Rev. D 35, 3366 (1987); 38, 1632(E) (1988).

[20] See, e.g., Novikov *et al.* (Ref. 3).

[21] The third χ_0 state, with mass somewhat smaller than that of $\Upsilon(4)$, may also lie below the $B\bar{B}$ threshold. We neglect this state in our treatment since no information for this state is available in the literature. Its effect can be inferred from analogy with the other two χ_0 states.

[22] Particle Data Group, G. P. Yost *et al.*, Phys. Lett. B 204, 1 (1988).

[23] S. Jacobs, M. G. Olsson, and C. J. Suchyta III, Phys. Rev. D 33, 3338 (1986); 34, 3536(E) (1986).

[24] S. N. Gupta, W. W. Repko, and C. J. Suchyta III, Phys. Rev. D 39, 974 (1989).

[25] R. Barbieri, R. Gatto, R. Kögerler, and Z. Kunszt, Phys. Lett. 57B, 455 (1975).

[26] W. Celmaster, Phys. Rev. D 19, 1517 (1979).

[27] In this paper we use the lowest-order formula for the QCD running coupling with $N_f = 4$.

[28] R. Barbieri, R. Gatto, and E. Remiddi, Phys. Lett. 106B, 497 (1981); W. Buchmüller, Y. J. Ng, and S.-H. H. Tye, Phys. Rev. D 24, 3003 (1981).

[29] This is due to the fact that θ is defined as the (complex) angle between the physical-Higgs-boson-like state and the unmixed Higgs-boson state. Had we defined it, e.g., as the angle between the lighter physical state and the unmixed Higgs boson, this change of sign would not have occurred, as discussed in Appendix B.

[30] The mass parameter m_b in the QCD calculation is defined as the position of the quark propagator in perturbation theory. It is thus appropriate to use the mass value determined from perturbative methods, not the mass in potential models nor the mass of the B meson. In this paper we use the value obtained in Ref. 11 from QCD sum rules. The same comment also applies to m_c.

[31] In principle one could try to multiply the b-loop contribution to the Higgs boson→gg amplitude with a function which approaches one for small mixing, but is smaller or even zero for large mixing. We did not use this approach since we do not know how severe the suppression should be, or how far it should extend.

[32] J. F. Gunion, G. L. Kane, and J. Wudka, Nucl. Phys. B299, 231 (1988).

[33] J. Lee-Franzini, in *Proceedings of the XXIV International Conference on High Energy Physics* (Ref. 1), p. 891; in '88 *Electroweak Interactions and Unified Theories,* proceedings of the XXIVth Rencontre de Moriond, Les Arcs, France, 1989, edited by J. Tran Thanh Van (Editions Frontières, Gif-sur-Yvette, 1989).

[34] The form of the helicity amplitudes Eq. (2.16) is fixed by the P-wave kinematics, except for the last mode $\Upsilon \to B^* \bar{B}^*$, for which two independent P-wave amplitudes exist. We assume the form of Yang-Mills coupling for the latter.

[35] A very similar result for charmonium resonances has been derived by A. De Rújula, H. Georgi, and S. L. Glashow, Phys. Rev. Lett. 37, 398 (1976).

[36] L. Ibáñez, Phys. Lett. 118B, 73 (1982); J. Ellis, D. V. Nanopoulos, and K. Tamvakis, *ibid.* 121B, 123 (1983); L. E. Ibáñez and C. López, Nucl. Phys. B233, 511 (1984); A. Bouquet, J. Kaplan, and C. A. Savoy, *ibid.* B262, 299 (1985).

[37] M. Olechowski and S. Pokorski, Phys. Lett. B 214, 393 (1988).

[38] UA2 Collaboration, P. Wells and CDF Collaboration, D. Baden, in '88 *Electroweak Interactions and Unified Theories* (Ref. 33).

[39] I. Antoniadis, J. Ellis, J. Hagelin, and D. V. Nanopoulos, Phys. Lett. B 208, 209 (1988). Similar patterns can also be obtained in orbifold models [H. P. Nilles (private communication)].

[40] J. Lee-Franzini, in *Proceedings of the XXIV International Conference on High Energy Physics* (Ref. 1), p. 1432.

[41] R. K. Ellis, I. Hinchliffe, M. Soldate, and J. J. van der Bij, Nucl. Phys. B297, 221 (1988).

[42] R. Gastmans, W. Troost, and T. T. Wu, Phys. Lett. B 184, 257 (1987); Nucl. Phys. B291, 731 (1987); B. Humpert, Phys. Lett. B 184, 105 (1987).

[43] M. Drees, Int. J. Mod. Phys. A 4, 3635 (1989).

[44] In contrast, the size of the theoretically less well understood region just above the open-flavor threshold, where even the QCD corrected prediction of the Higgs boson→$q\bar{q}$ decay

widths are unreliable, should be independent of m_q; it is related to the question at what energy scale perturbative QCD becomes reliable.

[45]K. Inoue, A. Kakuto, H. Komatsu, and S. Takeshita, Prog. Theor. Phys. **67**, 1889 (1982); R. A. Flores and M. Sher, Ann. Phys. (N.Y.) **148**, 95 (1983); J. F. Gunion and H. E. Haber, Nucl. Phys. **B272**, 1 (1986).